Measurements of the A_2^- and A_2^+ Mass Spectra

D. Bowen, D. Earles, W. Faissler, D. Garelick, M. Gettner, M. Glaubman, B. Gottschalk, G. Lutz, J. Moromisato,* E. I. Shibata, Y. W. Tang, and E. von Goeler
Northeastern University at Boston, Boston, Massachusetts 02115†

and

H. R. Blieden, G. Finocchiaro, J. Kirz,‡ and R. Thun
State University of New York at Stony Brook, Stony Brook, New York 11790§
(Received 8 April 1971)

Observations of the mass distribution of the A_2 meson produced in the reaction $\pi p \to A_2 p$ are reported. The A_2's were observed using a missing-mass technique. Measurements were made with 5- and 7-GeV π^- as well as 5-GeV π^+ beams. For each beam setting more than 17 000 A_2's above background were observed with $0.20 \leq |t| \leq 0.29$ GeV^2. The A_2 peaks are well described by a Breit-Wigner shape, whereas the dipole mass formula does not fit the data.

The CERN missing-mass–spectrometer group, CMMS, has performed several experiments[1,2] which show that the A_2 meson does not possess the usual Breit-Wigner shape, but instead is a double-peaked structure best described by a dipole mass formula. Subsequent experiments[2-7] have also examined the A_2 mass spectrum in detail. Some of these experiments[3,4] favor a dipole shape. In other experiments,[5-7] in which no dipole-like shape was found, the A_2 was observed under conditions differing from those of the CMMS experiments and thus do not necessarily contradict the CMMS findings. We report here[8] data obtained using a missing-mass technique to study the reaction $\pi p \to A_2 p$ in a similar manner and in the identical kinematic region as in the original CMMS experiments. Our data are well described by the Breit-Wigner formula and are inconsistent with a dipole shape.

The detector arrangement is shown in Fig. 1. The pion beam was produced by the slow external proton beam of the Brookhaven National Laboratory (BNL) alternating-gradient synchrotron. The recoil protons were detected by an easily rotatable telescope consisting of four wire spark chambers followed by five identical proton detectors which subdivided the vertical aperture. Each proton detector had an entrance aperture of 11.5×61.0 cm^2 located about 1.6 m from the target, and each consisted of a 1.27-cm-thick scintillation counter to measure proton dE/dx and time of flight, a 29.0-cm-deep plastic scintillation counter to stop the proton and measure its energy by the pulse-area method, and an anticoincidence counter to veto particles which did not stop.

A second spectrometer, consisting of wire spark chambers and trigger counters located before and after a magnet, was used to determine the production angles and momenta of particles produced in the forward direction. The magnet was placed about 5.8 m from the target. This spectrometer, having a momentum resolution of 1% full width at half-maximum (FWHM) at 5 GeV, detected primarily elastically scattered π's.

For each event, the mass of the charged boson is calculated from three measured kinematic quantities: the beam-particle momentum, the recoil-proton production angle, and the recoil-proton kinetic energy. In calibrating the scales and determining the resolutions associated with the measurements of these three kinematic quan-

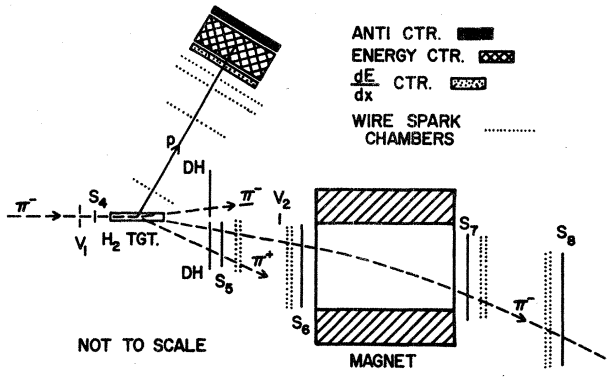

FIG. 1. Detector arrangement. The symbols S_1, $S_2, \cdots, S_8$ label aperture-defining scintillation counters, V_1 and V_2 label veto counters, and *DH* labels the decay hodoscope. The beam enters the detector region from the left after traversing a threshold Cherenkov counter, for π identification, and three beam hodoscopes which determined the momentum, angles, and lateral position of the incident particle at the hydrogen target. For the charged-boson missing-mass data, the trigger was π in, proton out.

Table I. Experimental resolutions (FWHM) and their contributions to the A_2-mass resolution. Proton resolutions are for $0.20 \leq |t| \leq 0.29$ GeV^2.

Beam momentum (GeV)	5	7
Proton production angular resolution (mrad)	8.6 ± 0.4	8.6 ± 0.4
Contribution to A_2-mass resolution (MeV)	13 ± 0.7	20 ± 1.0
Proton energy resolution (MeV)	5.0 ± 1.0	5.0 ± 1.0
Contribution to A_2-mass resolution (MeV)	3.0 ± 0.5	1.0 ± 0.5
Beam-momentum resolution (MeV)	54 ± 2.0	61 ± 2.0
Contribution to A_2-mass resolution (MeV)	8.0 ± 0.4	6.4 ± 1.0
Total A_2-mass resolution (MeV) (M = 1.30 GeV)	16 ± 1.0	21 ± 1.0

tities the following studies were made.

(1) The production-angle scale was determined by surveying the detectors and verified by rotating the proton detector into the beam.

(2) Elastically scattered pions were detected in the magnetic spectrometer at the same time that the A_2 data were obtained. The trigger for these events was π in, π out. This constituted a continuous direct measurement and monitoring of the beam momentum and its resolution. The total beam-momentum resolution, given in Table I, is the result of these measurements and includes the effects of possible beam drifts.

(3) At frequent intervals throughout the data taking, missing-mass experiments were performed in which the proton detector was set at an angle where mainly protons from elastic pion scattering were detected. These measurements were obtained by moving the proton detector to an angle about 20° larger than the settings used for collecting the A_2 data. The energy calibration of the proton detectors was determined and monitored by requiring that in these missing-mass distributions the π peak from elastic events be centered at the pion mass. (The trigger for these events was π in, proton out.) In addition, during the recording of the 7-GeV A_2^- data, protons from the elastic reaction were also detected at the same time as the A_2 events and provided a simultaneous monitoring of the proton-detector energy calibrations.

(4) In order to determine accurately the A_2-mass resolution, elastic events were studied in which both the recoil proton and scattered π were detected.[9] From these data is was possible to extract independently both the proton angular resolution and the energy resolution which are listed in Table I. This measured value for the angular resolution agrees with the value calculated taking into account multiple scattering in the materials along the recoil-proton path[10] and is consistent with the observed widths of the π peaks mentioned in (3) above.

The A_2-mass resolutions determined from the measured angular and energy resolutions are 16 ± 1.0 MeV FWHM at 5 GeV and 21 ± 1.0 MeV FWHM at 7 GeV. As indicated in Table I, the A_2-mass resolution is dominated by the proton angular resolution. The effects of drifts and possible systematic errors in the beam- and proton-energy calibrations are included in the stated resolutions and are negligible effects in this experiment. The measured A_2-mass resolutions compare favorably to the resolution of the CMMS 6- and 7-GeV A_2 data.[11]

A total of 8.5 million triggers (π in, proton out) was recorded for the three types of incident beams. All of the events were analyzed, and about half of them survived geometric reconstruction. In analyzing these data, further selections were made: (a) The production point of the event was restricted in order to exclude events from the target windows and walls. (b) To exclude protons which suffered a nuclear interaction in the proton-stopping scintillator, consistency between the measured proton energy and both its measured time of flight and measured dE/dx was required. (c) The position of the event extrapolated to the rear of the proton-stopping counter was restricted to insure that all of the stopping energy of the proton was contained in the counter. (d) In order to have a direct comparison with the CMMS data,[1] only events with proton four-momentum–transfer squared $0.20 \leq |t| \leq 0.29$ GeV^2 were kept. (In this experiment $t = -2m_p T_p$, where m_p is the mass of the proton and T_p is the proton kinetic energy.)

Mass distributions were examined for each of the proton detectors, separately, and for small intervals of proton energy. Fits to these data showed that the A_2 mass, width, and signal-to-background ratio at a single beam setting were independent of the proton detector which observed the events. The A_2 mass and width also were ob-

served to be independent of $|t|$ (within errors).

For the elastic-scattering data, the absolute cross sections and their $|t|$ dependences were determined. These elastic-scattering data provide a check on the event-selection criteria, the geometrical-detection-efficiency corrections, and the nuclear-absorption correction. In the interval $0.20 \leq |t| \leq 0.29$ GeV^2, the measured cross sections agree well (±10%) with published values.[12]

The A_2 mass distributions obtained at each value of beam momentum are shown in Figs. 2(a)-2(c).[13] In these figures, the calculated detection efficiencies[14] and the number of events divided by the calculated detection efficiencies are plotted versus mass. These spectra represent about 28 000, 24 000, and 17 000 detected A_2 mesons above background at 5 (π^-), 5 (π^+), and 7 (π^-) GeV, respectively, and have, at the A_2 peaks, a statistical precision of better than 3% per 5-MeV bin.

Fits to the data were made using a function, consisting of a background term plus either a Breit-Wigner or a dipole distribution, folded with the experimental mass resolution. Both a linear and a linear plus quadratic mass dependence were used for background terms. The data were fitted from 1.10 to 1.50 GeV in order to constrain the background to be smooth over the entire region. The form for the Breit-Wigner distribution was $B(M,M_0,\Gamma)=[(M-M_0)^2+\frac{1}{4}\Gamma^2]^{-1}$, and for the dipole, $D(M,M_0,\Gamma)=[B(M_0,M,\Gamma)(M-M_0)]^2$. In fitting the data with the dipole formula, two different types of fits were used. In one, the width of the dipole was fixed at 28 MeV, the value reported by the CMMS group,[1] and the mass was allowed to vary. In the other, both the mass and width were allowed to vary. For each fit the χ^2 was determined for all the fitted points ($1.1 \leq M \leq 1.5$ GeV, 80 data points), χ_T^2, and for the "resonance" region ($1.22 \leq M \leq 1.38$ GeV, 32 data points), χ_R^2. The quantity χ_R^2 is more sensitive to the A_2 shape and less sensitive to the exact form of the background in the A_2 region than is χ_T^2.

The results of the fits are shown in Table II. *All of the A_2 peaks are well described by the Breit-Wigner shape and are inconsistent with dipole shapes*, regardless of the form of the background assumed. For the three types of beams, the A_2 masses are equal (within errors), as are the widths.

In Table II, the quantity Σ is approximately equal to the number of standard deviations by which our data favor a Breit-Wigner fit over a dipole fit. Thus, *all* the fits to our data favor a Breit-Wigner fit by more than ~4 standard deviations. The experiment as a whole clearly rules out a dipole shape for the A_2.

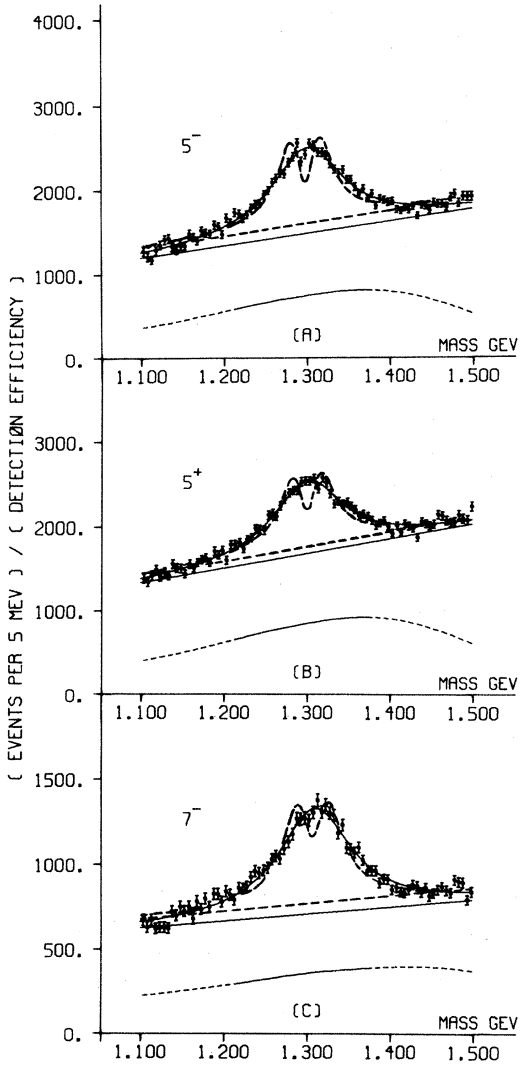

FIG. 2. (a)-(c) Mass spectra from 5 (π^-), 5 (π^+), and 7 (π^-) GeV, respectively. The solid lines through the data are the Breit-Wigner fits, and the solid straight lines beneath the data are the associated fitted linear backgrounds. The dashed lines in the region of the data are the dipole fits ($\Gamma_{\text{dipole}} = 28$ MeV, fixed) and their associated linear backgrounds. The calculated detection efficiencies versus mass are shown (arbitrary units) as dashed lines ($1.10 \leq M \leq 1.22$ GeV and $1.38 \leq M \leq 1.50$ GeV) and as solid lines ($1.22 \leq M \leq 1.38$ GeV, "resonance" region). The detection efficiencies have been normalized so that at $M = 1.300$ GeV the ordinates on the graphs indicate the actual number of events detected in the experiment per 5-MeV bin.

Table II. Results of the fits. The data are fitted over the interval $1.1 \leq M \leq 1.5$ GeV with a Breit-Wigner (B) [or a dipole (D)] distribution plus a linear (L) or linear plus quadratic (Q) background. The number of degrees of freedom for the entire interval $1.1 \leq M \leq 1.5$ GeV is 75 for the L fits and 74 for the Q fits. χ_T^2 and χ_R^2 are the total χ^2 for the regions $1.1 \leq M \leq 1.5$ GeV and $1.22 \leq M \leq 1.38$ GeV, respectively. The quantity $\Sigma \equiv (\chi_D^2 - \chi_B^2)/(60)^{1/2}$ is the difference in χ^2 for the D and B fits for $1.22 \leq M \leq 1.38$ GeV divided by the approximate expected fluctuation in χ^2 for this mass interval. $P(\chi_R^2)$ is the probability of observing a χ^2 larger than χ_R^2, assuming χ_R^2 obeys a χ^2 distribution with 30 degrees of freedom. M_0, Γ, and R are, respectively, the resonance mass, width, and signal-to-background ratio (at $M = M_0$) given by the fits. The uncertainties listed with M_0 include the effects of possible systematic errors associated with determining this quantity. The errors listed with Γ are the statistical errors of the fits.

Resonance & Background Distribution Used	Beam Momenta[a] (GeV)	R	M_0 (MeV)	Γ (MeV)	χ_T^2	χ_R^2	Σ	$P(\chi_R^2)$
B+L	5^-	0.79	1299 ± 6	105 ± 5	114	31		4×10^{-1}
D+L	5^-		1299 ± 6	26 ± 1	368	238	27	3×10^{-34}
D+L[b]	5^-		1298 ± 6	28[b]	374	252	29	6×10^{-37}
B+L	5^+	0.52	1300 ± 6	99 ± 5	94	27		6×10^{-1}
D+L	5^+		1300 ± 6	25 ± 1	271	179	20	4×10^{-23}
D+L[b]	5^+		1300 ± 6	28[b]	283	200	22	5×10^{-27}
B+L	7^-	0.89	1309 ± 4	103 ± 5	100	29		5×10^{-1}
D+L	7^-		1308 ± 4	27 ± 1	231	135	14	3×10^{-15}
D+L[b]	7^-		1308 ± 4	28[b]	231	138	14	9×10^{-16}
B+Q	5^-	0.82	1300 ± 6	118 ± 9	109	30		5×10^{-1}
D+Q	5^-		1298 ± 6	23 ± 1	243	114	11	1×10^{-11}
D+Q[b]	5^-		1298 ± 6	28[b]	281	166	18	9×10^{-21}
B+Q	5^+	0.61	1300 ± 6	113 ± 9	89	27		6×10^{-1}
D+Q	5^+		1301 ± 6	22 ± 1	195	94	9	2×10^{-8}
D+Q[b]	5^+		1299 ± 6	28[b]	234	146	15	3×10^{-7}
B+Q	7^-	0.81	1309 ± 4	96 ± 9	99	29		5×10^{-1}
D+Q	7^-		1309 ± 4	23 ± 1	138	58	4	2×10^{-3}
D+Q[b]	7^-		1308 ± 4	28[b]	159	87	7	2×10^{-7}

[a]The superscript on the beam momentum designates the charge of the incident pion.
[b]For these fits the dipole width was fixed at 28 MeV.

To investigate the significance of the disagreement between our results and the CMMS 6- and 7-GeV results,[1] our mass distribution for the 7-GeV beam [Fig. 2(c)] was compared directly to that of CMMS. This comparison indicates that in the region of the A_2 peak, where $1.29 \leq M \leq 1.31$ GeV, the data from the two experiments differ by a total of more than a 7 standard deviations.[15]

We gratefully acknowledge the cooperation and assistance of many people; in particular, W. Armstrong, C. Boyer, B. Cairns, R. Mustard, and the staffs of the BNL alternating-gradient synchrotron and on-line data facility, and the BNL and Northeastern University computing centers. The loan of equipment to us by Carnegie-Mellon University (Professor R. Edelstein), Cornell University (Professor J. Orear), and the Brookhaven Physics Department (Dr. G. Collins and Dr. S. Lindenbaum) is also gratefully acknowledged. We thank Professor R. Weinstein for his important contributions throughout the course of the experiment.

*On leave of absence from the University of San Marcos, Lima, Peru. Supported in part by a Ford Foundation Fellowship.

†Work supported in part by the National Science Foundation under Grants No. GP9217 and No. GP25307.

‡Alfred P. Sloan Foundation Fellow.

§Work supported in part by the U. S. Atomic Energy Commission.

[1]G. Chikovani *et al.*, Phys. Lett. 25B, 44 (1967).

[2]For a summary of and for a list of references to the CMMS work and other A_2 experiments see P. Schübelin, Phys. Today 23, 32 (1970). See also the reviews contained in *Experimental Meson Spectroscopy*, edited by C. Baltay (Columbia U. Press, New York, 1970).

[3]M. Aguilar-Benitez *et al.*, Phys. Lett. 29B, 62 (1969).

[4]M. Basile *et al.*, Lett. Nuovo Cimento 4, 838 (1970).

[5]M. Alston-Garnjost *et al.*, Phys. Lett. 33B, 607 (1970).

[6]G. Grayer *et al.*, Phys. Lett. 34B, 333 (1971).

[7]K. J. Foley *et al.*, Phys. Rev. Lett. 26, 413 (1971).

[8]A more detailed report of this work has been submitted for publication in "Phenomenology in Particle Physics 1971," edited by C. Chiu, G. Fox, and A. Hey (California Institute of Technology, Pasadena, Calif., to be published).

[9]From these data absolute values of the incident beam momenta are also obtained using measurements of the scattering angles only. The values agree to within

0.3% with the values deduced using the magnetic spectrometer.

[10]The material in the path of the recoil proton, contributing to multiple scattering (ms), consisted of 2.9×10^{-3} radiation lengths (rl) of material perpendicular to the π beam (1.5×10^{-3} rl of liquid H_2 plus 1.4×10^{-3} rl of other material) plus 0.8×10^{-3} rl perpendicular to the proton line of flight. For 20% of the events, an additional average of 5.6×10^{-3} rl of Cu wire of the first spark chamber must be added. The angular measuring accuracy of the spark chambers plus the uncertainty in the incident beam angle was 3 mrad FWHM. The ms calculations are based on the work of R. Diebold, SLAC Report No. RD-11, 1967 (unpublished).

[11]The total "high-resolution" data in Ref. 1, Fig. 4, are compiled from samples with resolutions of 26, 18, and 16 MeV. We estimate the effective resolution of this sample to be 20 MeV FWHM.

[12]C. T. Coffin *et al.*, Phys. Rev. 159, 1169 (1967).

[13]The fluctuation in the 5-GeV (π^-) data [Fig. 2(a)] just below $M=1.300$ GeV has been investigated by rebinning these data with the bin origins shifted by 2.5 MeV. Upon rebinning, the fluctuation becomes significantly reduced.

[14]The detection efficiencies are calculated assuming a production cross section of the form $d^2\sigma/dMdt = G(M)\times\exp(-B|t-t_M|)$, where $G(M)$ is the total cross section per unit mass for production of particles with an effective mass M, and t_M is the minimum t possible for mass M. The value of $B=8$ GeV^{-2}, which represents well the t dependence of all the data for $1.1\leq M\leq1.5$ GeV, was used in the calculations.

[15]A special selection of our 7-GeV data was also made to more closely approximate the exact conditions of the CMMS experiment. For this selection, data were chosen in which one, two, or three charged particles were detected in the hodoscope covering a large portion of the solid angle in the forward direction. Fits to these data favor a Breit-Wigner shape by ~12 standard deviations (linear background).

Experimental Limits on the Decays $K_L^0\to\mu^+\mu^-$, e^+e^-, and $\mu^\pm e^\mp$†

Alan R. Clark, T. Elioff,* R. C. Field, H. J. Frisch, Rolland P. Johnson, Leroy T. Kerth, and W. A. Wenzel
Lawrence Radiation Laboratory, University of California, Berkeley, California
(Received 9 April 1971)

We have performed a search at the Bevatron for the decays $K_L^0\to\mu^+\mu^-$, e^+e^-, and $\mu^\pm e^\mp$ with a double magnetic spectrometer using wire spark chambers. Over 10^6 observed $K_L^0\to\pi^+\pi^-$ decays determine the normalization for the di-lepton decay modes. No e^+e^- or $\mu^\pm e^\mp$ events were observed. For each of these decays the upper limit on the branching ratio relative to all modes is 1.57×10^{-9} (90% confidence level). For the decay $K_L^0\to\mu^+\mu^-$, the limit is 1.82×10^{-9} (90% confidence level).

The $K_L^0\to\mu^+\mu^-$ decay is generally considered to be a sensitive test of the existence of weak neutral currents. This decay should also occur via higher-order weak interactions.[1] Current algebra techniques have been used to relate the rates for $K^+\to\mu^+\nu$ and the second-order weak process $K_L^0\to\mu^+\mu^-$.[2] An upper bound on the weak interaction cutoff then follows from the experimental limit on $K_L^0\to\mu^+\mu^-$.

The $K_L^0\to l^+l^-$ decays should also be induced by electromagnetic interactions.[3] Using the measured $K_L^0\to\gamma\gamma$ rate[4] and assuming only the two-photon intermediate state, branching ratios of approximately 10^{-8} have been predicted from various models for the $K_L^0\to\mu^+\mu^-$ decay.[5] Neglecting the contributions from off-mass-shell photons, one can derive a "unitarity" lower limit of 6×10^{-9} for this decay. However, other intermediate states may destructively interfere, producing a limit lower than that predicted by the two-photon state alone. Martin, de Rafael, and Smith[6] have estimated that contributions from the $\pi\pi\gamma$ and 3π intermediate states can lower the rate by at most 20%.

The $K_L^0\to e^+e^-$ rate is suppressed by a factor of $(m_e/m_\mu)^2$ relative to the $K_L^0\to\mu^+\mu^-$ rate in weak models which use $V-A$ and also in electromagnetic models. The $K_L^0\to e^\pm\mu^\mp$ rates are not predictable from any known interaction. Limits on these decays (which violate separate lepton-number conservation) can be compared with limits on $\mu^\pm\to e^\pm\gamma$ or $\mu^\pm\to e^\pm e^+e^-$. Table I shows these limits and previously published limits on the various di-lepton decay modes of the K_L^0.

Figure 1 shows the plan view of the detection apparatus.[7] The 6-m-long decay volume began 7.6 m from the production target in the Bevatron external proton beam. The 0.8-msr beam yielded $\sim6\times10^5$ K_L^0's in the momentum range 0.8-3.2 GeV/c for 6×10^{11} protons on the target. The